# Environmental Patterns Associated with Active and Inactive Caribbean Hurricane Seasons

MARK R. JURY

*Physics Department, University of Puerto Rico, Mayaguez, Puerto Rico*

DAVID B. ENFIELD

*NOAA/AOML, Miami, Florida*

(Manuscript received 14 April 2009, in final form 30 September 2009)

ABSTRACT

This study of hurricanes passing through the Caribbean in the 1950–2005 period reveals that seasons with more intense hurricanes occur with the onset of Pacific La Niña events and when Atlantic SSTs west of Africa are above normal. Composites of NCEP reanalysis fields with regard to Caribbean hurricanes reveal development of an anomalous equatorial Atlantic zonal overturning circulation (upper easterly/lower westerly) that shifts toward the Caribbean coincident with a westward spread of the cold tongue in the east Pacific. Ocean–atmosphere coupling is promoted through interaction of the southern Hadley cell and the Atlantic ITCZ. A heat budget analysis suggests that evaporation governs SSTs in the major development region (MDR) and near Venezuela, but the signal is weak prior to May. Using the knowledge gained, statistical algorithms are developed to predict Caribbean hurricanes at seasonal lead times. These make use of equatorial Pacific SST, subtropical Atlantic SST, and the zonal Walker cell over the Atlantic.

## 1. Introduction

Climatic signals have been found to play a role in shifting the probability of occurrence of hurricanes throughout the tropics. Influential signals with respect to Atlantic hurricanes include the interannual Pacific El Niño–Southern Oscillation (ENSO) and associated changes in zonal wind shear (Gray 1984; Klotzbach and Gray 2003; Aiyyer and Thorncroft 2006) and tropical Atlantic SSTs that affect both shear and tropospheric stability on interannual to multidecadal time scales (Goldenberg et al. 2001; Wang and Enfield 2003; Wang et al. 2006; Wang and Lee 2007; Wang et al. 2007). Other factors that may affect Atlantic hurricanes include the stratospheric quasi-biennial oscillation (QBO), modulating hurricane abundance, and the North Atlantic oscillation (NAO), affecting hurricane tracks by distorting the subtropical anticyclone (Gray 1984; Elsner et al. 2006).

Climate–weather interactions are variable, and relationships between indices of regional circulations and hurricanes are unstable. This should be expected, considering the different time scales. A short-lived extreme event within a low-frequency envelope is unable to find constant ''traction.'' So, a degree of chaos is expected to reduce hurricane predictability, especially in the boreal summer ENSO transition season. Nonetheless, Klotzbach and Gray (2003) have uncovered many statistical predictors of Atlantic hurricane activity: 1) SST in the east Pacific as a measure of ENSO; 2) SST to the southwest of Europe, an index of the Atlantic subtropical ridge; 3) air pressure in the north tropical Atlantic as a measure of stability and trade winds; and 4) 500-hPa geopotential heights in the far north Atlantic, to reflect the jet stream and the influence of the NAO. Here, we have a closer look at tropical Atlantic SSTs.

Links between climate variability and Atlantic hurricanes have been investigated using field data on regional SST and circulation anomalies and on hurricane statistics on position and intensity. Aiyyer and Thorncroft (2006) confirmed the enhancement of Atlantic hurricanes by anomalous tropical upper (lower) easterly (westerly) flow. Increased upper anticyclonic shear, which aids hurricane outflow, is associated with the La Niña phase of

*Corresponding author address:* Mark R. Jury, Physics Department, University of Puerto Rico, Mayaguez, PR 00681.
E-mail: mark.jury@upr.edu

DOI: 10.1175/2009JCLI3201.1

ENSO. A rapid teleconnection occurs as the large-scale, wavenumber-one divergent circulation shifts, spinning up anomalous Pacific and Atlantic Walker cells (Yeshanew and Jury 2007). The zonal overturning controls a significant portion of African and South American climate variability (Hastenrath 2000; Jury 2003; Cook et al. 2004). A factor that sometimes overrides the Pacific ENSO influence is tropical Atlantic SST, with anomalies driven by evaporation feedback (Xie and Philander 1994; Carton et al. 1996; Chang et al. 1997) and by the Amazon convection or the NAO (Mestas-Nuñez and Enfield 2001; Enfield et al. 2006). The Atlantic influence on climate is potentially connected with the Pacific. An example of the interocean linkage is the way ENSO affects Atlantic SST (Enfield et al. 2006), whereas the latter subsequently affects hurricanes (Wang et al. 2006). Nevertheless, Wang et al. (2006) clearly demonstrate that much of the variability of the Atlantic warm pool is unrelated to Pacific SST.

Our work here aims to determine what is unique about the regional environment that produces seasons with more intense hurricanes passing through the Caribbean (Elsner and Jagger 2008). For this, we contrast the relative importance of Atlantic and Pacific forcing, to resolve whether these drivers cooperate or lag each other. We define Caribbean hurricanes as those reaching hurricane intensity within the region south and east of Key West, Florida (10°–25°N, 82°–50°W), including those passing from Africa through the major development region (MDR; 10°–20°N, 25°–50°W) and those forming near the Antilles Islands. We seek to establish the Western Hemisphere patterns driving Caribbean hurricane variability following on the work of previous all-Atlantic studies (Goldenberg et al. 2001; Wang et al. 2006; Wang and Lee 2007; Wang et al. 2007). We seek to determine whether Caribbean hurricanes respond to environmental forcing different than for hurricanes in the wider Atlantic basin, through consideration of composite maps of surface and atmospheric variables in ''active'' and ''inactive'' periods. The composites are analyzed ''before'' and ''during'' the season, to determine whether the signals derive from stationary or transient modes. Several questions will be addressed in the analysis of year-to-year variations of Caribbean hurricanes:

(i) What specific regional atmospheric circulation and ocean thermal signals are evident during active and inactive Caribbean hurricane phases?
(ii) Do the anomalous climate signals propagate across the tropics?
(iii) What are the leads/lags and covariability that relate to the prediction of Caribbean hurricanes at seasonal lead times?

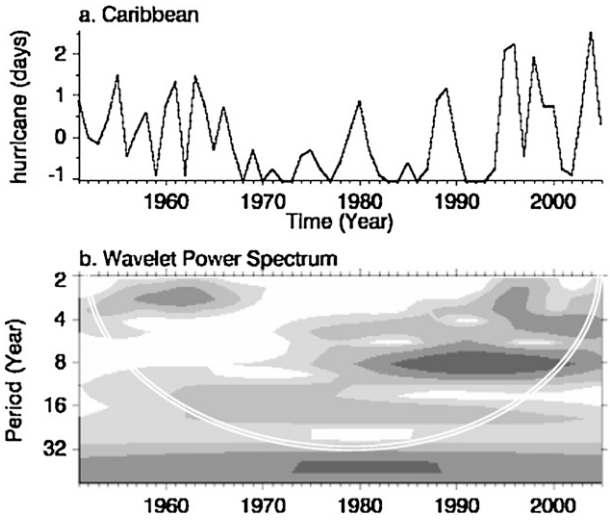


FIG. 1. (a) Number of days each year in the Caribbean region with hurricanes present in the July–October season. (b) Wavelet spectrum for the CHD index with power shaded at 20% intervals and cone of validity.

## 2. Data and methodology

Historical hurricane data extracted in 2006 from the Hurricane Research Division (HRD)–Atlantic Oceanographic and Meteorological Laboratory (AOML) Hurricane Database (HURDAT; available online at http://www.aoml.noaa.gov/hrd/data_sub/re_anal.html) were used to determine the number of days that hurricanes (Vmax $>$ 33 m $s^{-1}$) were present in the area 10°–25°N, 82°–50°W (southeast of Key West, Florida), which we shall adopt as our definition of Caribbean. The number of days each year was counted from the 6-hourly information and used to form a Caribbean hurricane days (CHD) time series shown in Fig. 1a. Our time series is consistent with the tropical cyclone index of Aiyyer and Thorncroft (2006), with a correlation of +0.77 over the period 1951–2005, significant at the 99% confidence limit. Possible trends in the HURDAT database resulting from secular changes in tropical cyclone detection techniques are discussed by Landsea et al. (2006) and Landsea (2007).

Relationships between the CHD time series and various regional environmental parameters and global indices were analyzed. Cross correlations exceeding 0.26 are considered significant at 95% confidence limit with 55 degrees of freedom (e.g., the autocorrelation at lag +1 yr is insignificant). Cycles within the CHD index time series were analyzed using wavelet transform via a Web site (available online at http://ion.researchsystems.com/). Years with high and low CHD are selected as described later and provide dates used in the spatial

TABLE 1. Contingency tables based on tercile classes of (top) AWP size and (bottom) N3.4 SST index vs hurricane activity measured by normalized hurricane days for the Caribbean (CHD) as defined in the text. Data are for August–October 1951–2005. Active seasons have CHD $\geq +0.50$; inactive seasons have CHD $\leq -0.75$; and other years are "neutral."

| | Small AWP | Neutral AWP | Large AWP | Row tot |
|---|---|---|---|---|
| Active | 2 | 7 | 10 | 19 |
| Neutral | 7 | 3 | 6 | 16 |
| Inactive | 9 | 8 | 3 | 20 |
| | Cool N3.4 | Neutral N3.4 | Warm N3.4 | Row tot |
| Active | 8 | 7 | 4 | 19 |
| Neutral | 4 | 7 | 5 | 16 |
| Inactive | 6 | 4 | 10 | 20 |

analyses that consider the pattern and strength of composite signals in the National Centers for Environmental Prediction (NCEP) reanalysis data before and during the hurricane season. The thermodynamic forcing is studied using National Oceanic and Atmospheric Administration (NOAA) extended SST and NCEP tropopause temperature fields. The kinematic forcing is analyzed using the wind field and its derivatives: velocity potential and streamfunction. To supplement the thermodynamic analysis, we calculate the ocean heat budget in the MDR (10°–20°N, 25°–50°W). We extend the kinematic analysis by considering the vertical structure of the Atlantic zonal circulation (Walker) cell and the patterns of upper- and lower-level velocity potential that helps characterize it. We investigate north–south shifts in the Atlantic ITCZ using NOAA satellite interpolated outgoing longwave radiation (OLR) data in the period since 1979, and we study east–west shifts in the regional circulation and SST gradients using Hovmöller analysis.

NCEP reanalysis composites are constructed for high and low hurricane seasons, based on the CHD index (Fig. 1a). We select the 10 highest hurricane years (1955, 1961, 1963, 1980, 1988, 1989, 1995, 1996, 1998, 2004) and 10 lowest hurricane years (1968, 1970, 1972, 1973, 1977, 1983, 1984, 1986, 1991, 1992).

Four-month seasonal composites are averaged for each group [e.g., March–June (or preseason or before) and July–October (or in-seasons or during)] using the Climate Diagnostics Center (CDC) Web site. For most variables, the fields are opposed and of similar strength for the high and low CHD groups. We therefore assume linearity of

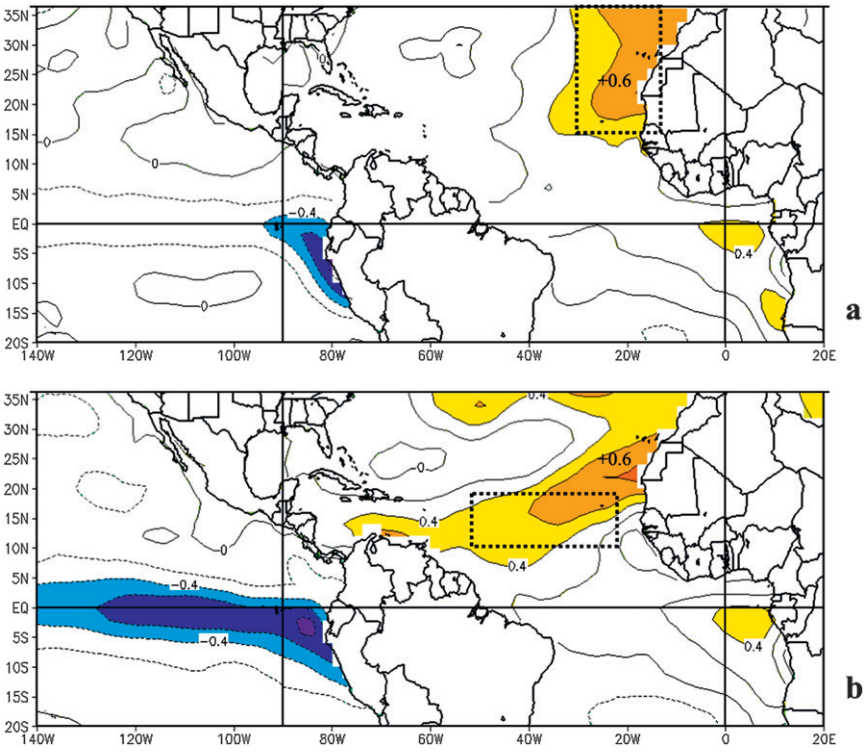


FIG. 2. (a) March–June (preseason) high minus low composite for SST in units of °C and (b) July–October (in-season) SST pattern. Box in (b) identifies the MDR for heat budget analysis. Box in (a) refers to predictor used in model. Only regions of higher amplitude are shaded here and in the following figures.

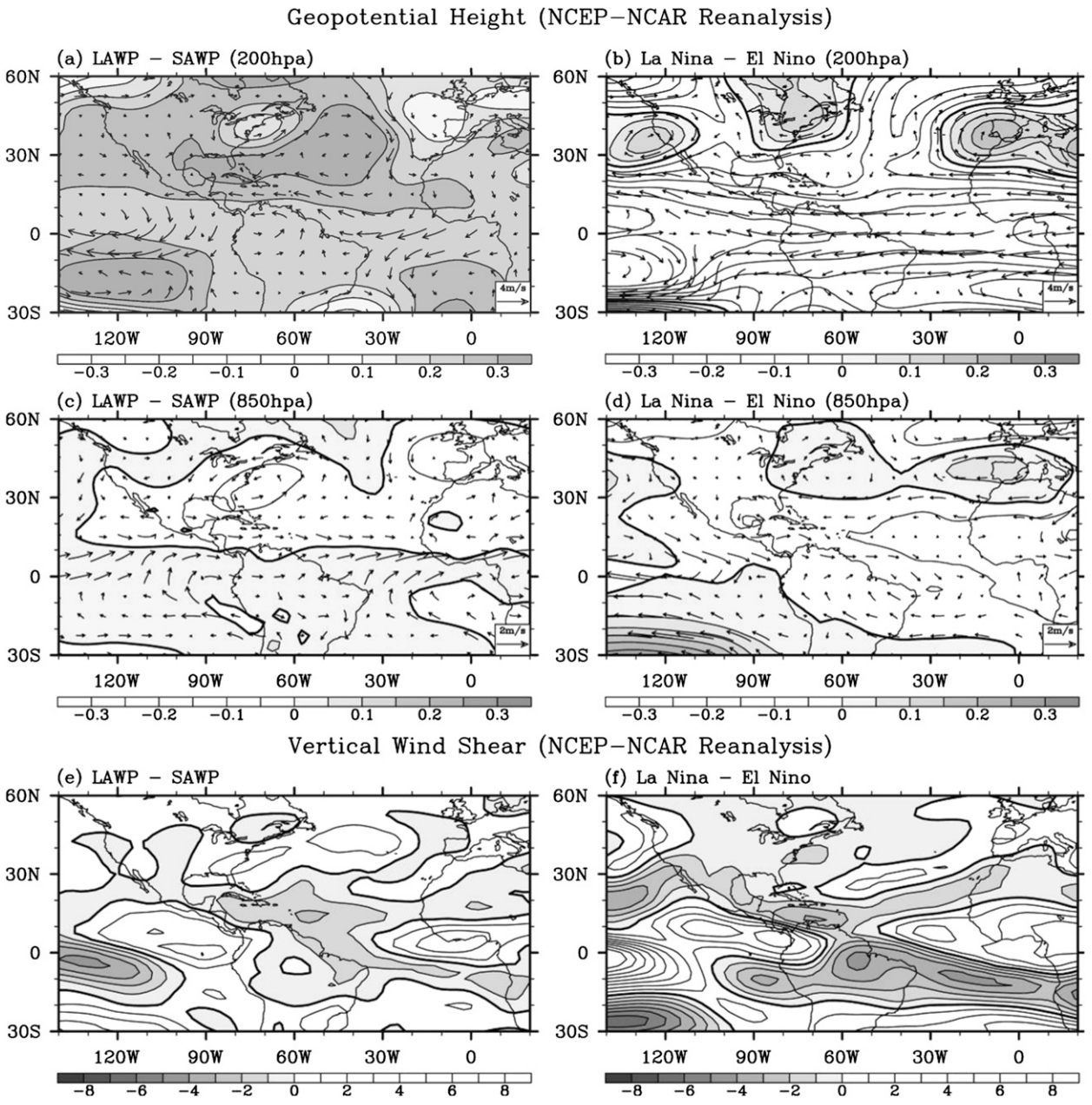


FIG. 3. Composite June–November maps of (left) years with highest tercile of AWP (LAWP) size minus lowest tercile (SAWP) and (right) for the lowest tercile of SST in the Niño-3 region minus the highest tercile for (a),(b) 200- and (c),(d) 850-hPa geopotential height and winds and for (e),(f) magnitude of zonal wind shear between 200 and 850 hPa, where easterly is shaded.

environmental controls and reduce the analysis by subtracting composite fields of the low group from the high group, producing difference maps. These point us to key areas for evaluation of signals (where differences exceed one standard deviation) and extraction of predictor variables. Statistical constraints require us to limit the number of candidate predictors to a minimum. Consideration of a wider range of predictors that will generate artificial skill is avoided. We seek to understand why some variables are more influential through investigation of the processes involved: MDR heat budget, vertical wind shear, and zonal and meridional propagation.

We analyze the ocean heat budget by extracting the various surface flux components from NCEP via the Nomads Web site averaged over the MDR box, as anomalies with a 3-month running mean applied. It is known that the reanalysis flux fields are inaccurate in the early years (Yu et al. 2004), so we extract duplicate flux

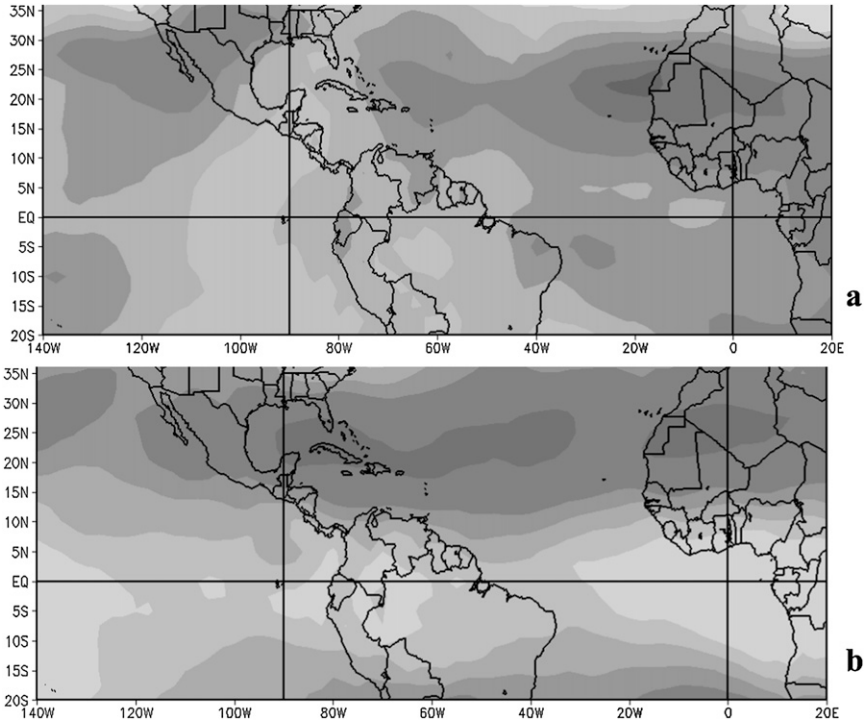


FIG. 4. (a) Preseason high minus low composite for tropopause temperature and (b) in-season tropopause temperature pattern, with gray shading from darkest −1.2 to lightest +1.2 at 0.3°C intervals.

components in the same manner from the DaSilva (ship only) dataset via the International Research Institute for Climate and Society (IRI) Climate Library Web site (available online at http://iridl.ldeo.columbia.edu/SOURCES/.DASILVA/). Following comparisons, adjusted flux time series were created by averaging the two datasets.

To estimate the oceanic entrainment $w$ effect on SST, the reanalysis wind stress curl was extracted in the MDR together with the vertical temperature gradient below the mixed layer from the Simple Ocean Data Assimilation (SODA) University of Maryland (UMD) ocean reanalysis data via the IRI Web site. Cross comparisons were made between the monthly values from SODA and the climatological mean values from the Levitus ocean atlas (http://iridl.ldeo.columbia.edu/SOURCES/.NOAA/.NODC/.WOA05/). In this way, wind-driven vertical motions were accounted for in our budget. To estimate the ocean's advective $u$ effect on SST,SODA-estimated ocean currents averaged over the mixed layer depth (upper 35 m) were multiplied by the horizontal temperature gradient.

The ocean heat budget equation used is $d\mathrm{SST} = (\mathrm{Qnet}\ dt/\rho \mathrm{Cp}\ dz) + w\ dt(d\mathrm{Te}/dz) + U\ dt(d\mathrm{Tm}/dx)$. The net flux Qnet = Qs − Ql − Qe − Qh [i.e., the net solar insolation Qs (received in the mixed layer) minus the longwave radiation Ql, the evaporative flux Qe, and the sensible heat flux Qh. Here, $\rho$ is the water density, Cp is the specific heat of water, and $dz$ is the mixed layer depth. Vertical motion $w = T\mathrm{curl}/\rho f$, the wind stress curl: here, calculated similar to vorticity, $f$ is the local Coriolis parameter. Here, Qs received in the mixed layer is estimated from Enfield and Lee (2005), Te is the entrainment temperature at the base of the mixed layer, and Tm is the mixed layer temperature. All components of the heat budget vary freely, but some are less well specified by data, such as currents and thermal stability. Here, $dt$ is one month, and all input variables are 3-month-smoothed anomalies (seasonal cycle removed). As mentioned earlier, the flux terms derive from NCEP reanalysis and DaSilva datasets, whereas the remaining terms are derived from the SODA UMD ocean reanalysis, using a methodology consistent with Jury et al. (2002). Considering the uncertainties involved, we employ composite analysis of calculated and observed values for high and low hurricane years to understand the thermodynamic drivers in the MDR.

## 3. Results

### a. Time series

The CHD index (Fig. 1a) exhibits a number of years with more than a dozen hurricane days, and a similar

number of years with less than one. The wavelet spectrum reveals two dominant signals in the CHD index: a 3-yr cycle in the period 1950–70 and an 8-yr cycle thereafter (Fig. 1b). The 3-yr cycle is consistent with a high-frequency component of global ENSO, found across the tropical Indian and Pacific Oceans in the 1950s and 1960s. The 8-yr cycle may be attributable to a decadal component of ENSO that influences SST variability in the Caribbean and MDR (Jury 2009).

There is a single multidecadal cycle in the data, with high CHD years at the beginning and end of the record. Longer datasets confirm the persistence of this cycle (Goldenberg et al. 2001; Nyberg et al. 2007) consistent with the Atlantic multidecadal oscillation (AMO). In Table 1, we note that all of the low years fall in the cool phase of the AMO between the mid-1960s and 1995; only three of the high years fall in that period, all other high years occur in AMO warm phases prior to 1965 or after 1994. Two of the high years occurring in the AMO cool phase correspond with the 1988/89 La Niña. Hence, the distribution of CHD counts confirms a multidecadal relation of Caribbean activity to Atlantic SSTs similar to that found by Goldenberg et al. (2001) for the broader tropical cyclone domain.

Simultaneous correlations between the CHD index and various known climatic indices available from CDC reveal that only a few achieve significance: Pacific Niño-1 and Niño-3 SSTs, rainfall over the southwestern United States and India, the MJO (intraseasonal index), and the AMO. The Pacific connection with Atlantic hurricanes is well known (Goldenberg and Shapiro 1996, etc.), and it is related to upper westerly shear anomalies over the tropics that influence convective outflows. Maloney and Hartmann (2000) have identified how the MJO influences hurricane activity, through surges of low-level westerlies that reach the Caribbean and increase cyclonic wind vorticity and hurricane activity. Outflow from the Indian monsoon initiates a tropical easterly jet over North Africa, generating perturbations that drift westward toward the Caribbean (Hopsch et al. 2007). The AMO correlation is consistent with the analysis of Goldenberg et al. (2001) and probably reflects the recurrence of large or small Atlantic warm pools (Wang et al. 2008).

Pairwise zero-lag correlations between the CHD index and various environmental indices in the Caribbean region (10°–24°N, 45°–82°W but 5°–15°N for zonal winds), yield significant values (in descending order): zonal wind at 925 hPa (+.66), sea level pressure (−0.62), streamfunction at 850 hPa (+.50), zonal wind at 200 hPa (−0.40), SST (+.39), and precipitable water (+.38). The kinematic variables seem to outshine the thermodynamic variables, as highlighted later. These relationships are consistent with the analysis of Knaff (1997).

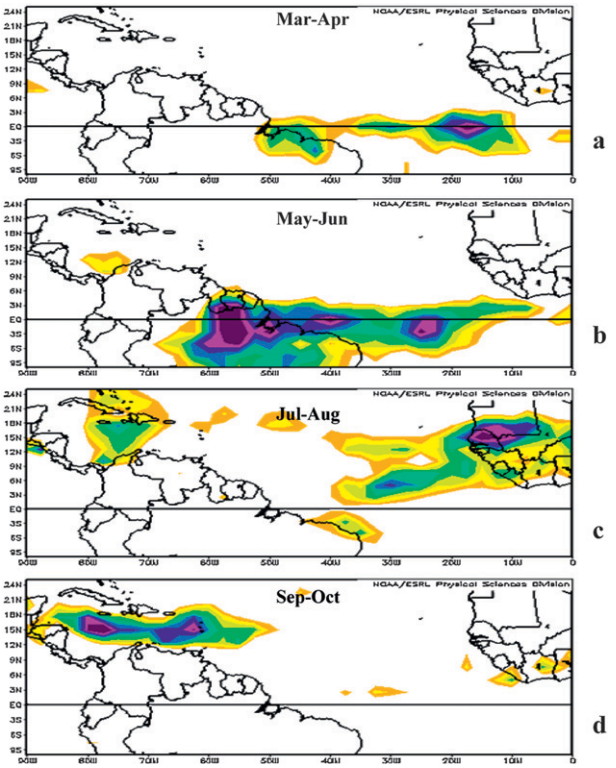


FIG. 5. (a)–(d) Sequence of high minus low composite satellite OLR for cases in the satellite era. Values from −4 to −12 W $m^{-2}$ are shaded.

Swanson (2008) points out that some of the contemporaneously correlated variables (e.g., winds and pressure) are ''contaminated'' by the presence of the hurricanes themselves in the region of greatest occurrence (MDR). Hence, although the physical influence of high vertical wind shear in discouraging convective development of tropical cyclones is well understood, the corresponding correlations found here may be inaccurate upper bounds and should be treated qualitatively rather than quantitatively. A similar caveat applies to the contemporaneous composite distributions discussed later. This should not be a problem, however, when comparing the summer CHD index to the indices and composites for the spring season.

The size of the Atlantic warm pool (AWP; defined as SST > 28.5°C) has been found to be associated with vertical wind shear and moist static energy over the main development region of Atlantic hurricanes (Wang et al. 2006, 2007). In Table 1, we provide a tercile contingency analysis that shows that the number of Caribbean hurricane days is significantly greater (less) in years with large (small) AWP over the period 1951–2005. A total of 53% of years with large warm pools had active seasons, whereas the frequency of inactive seasons is only 16%.

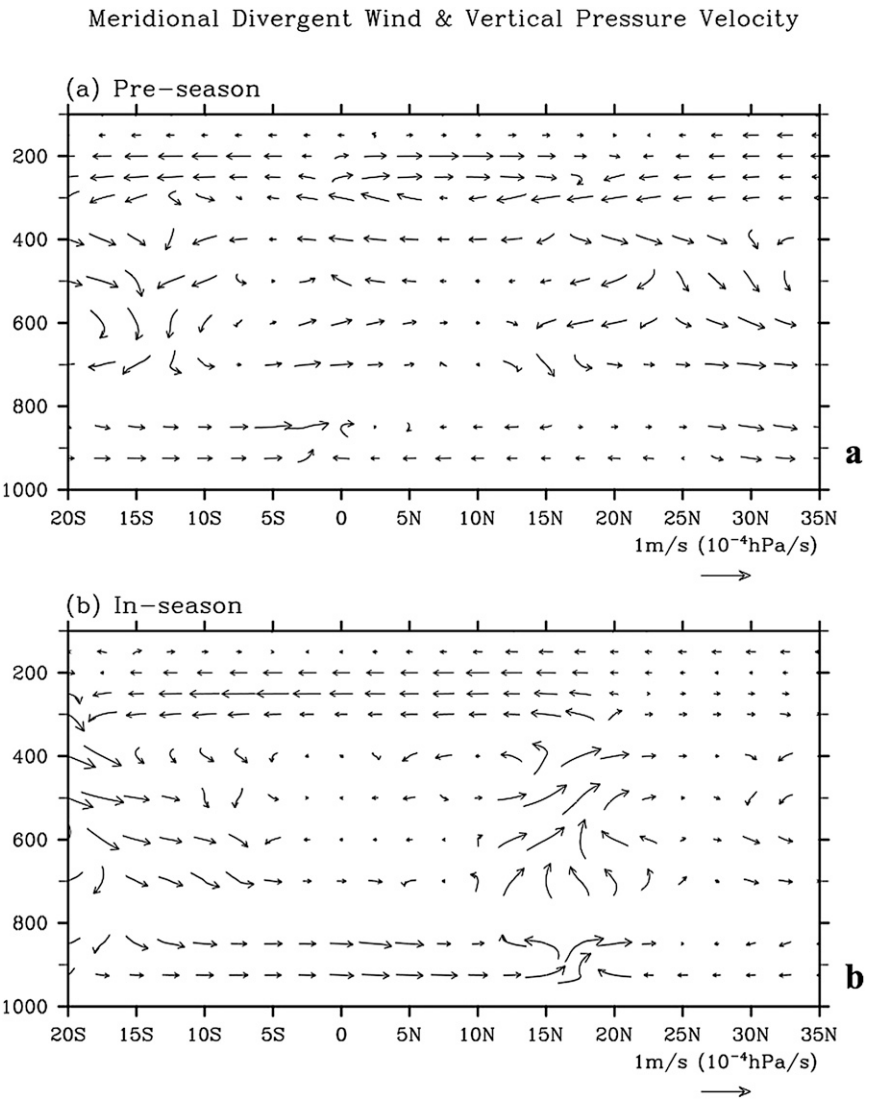


FIG. 6. Vertical north–south section composite over the MDR (25°–50°W) of divergent component of meridional wind and vertical motion (inverted omega scaled up × 100) during (a) preseason and (b) in-season. The vector key is given.

For years with small AWPs, the dichotomy is similar but favors inactive seasons.

The contingency table for hurricane days against the Niño-3.4 (N3.4) SST index shows the conventionally understood inverse relationship between equatorial Pacific SST and contemporaneous Atlantic hurricane activity (Table 1). Roughly half of warm episodes since 1950 are associated with inactive Caribbean hurricane seasons as opposed to about 20% with active seasons, which is comparable to the impact of small AWP. However, the occurrence of cool conditions in the Pacific is less skillful in anticipating active seasons than is a large AWP. As with AWP, ENSO influences vertical shear in the tropical Atlantic, accounting for an inverse relationship. However, unlike for AWP, the thermodynamic reaction to ENSO is such that the kinematic effects of shear appear to be partially offset, producing a lower comparative skill.

### *b. Composite thermodynamic structure*

Composite maps for the thermodynamic variables are presented here. The SST maps before and during the season reveal warming initially in the upwelling region off the coast of North Africa and west of Portugal (Figs. 2a,b). This warming spreads toward the Caribbean from May to September, crossing the MDR where African perturbations enter the tropical Atlantic (Hopsch et al. 2007). The difference between the high and low years is only 0.6°C, compared to a mean standard deviation for

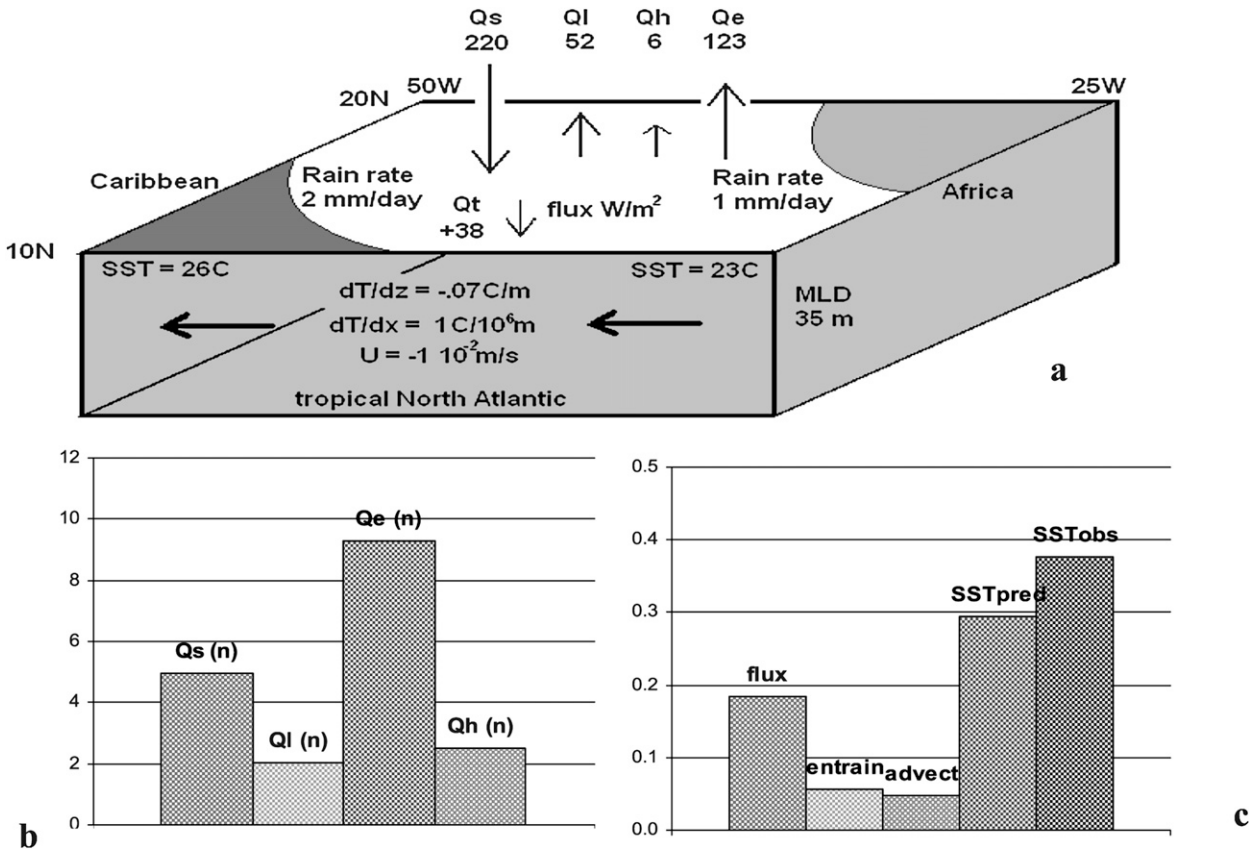


FIG. 7. (a) Climatology of the MDR heat budget indicating the key features in the March–October season; (b) interannual standard deviation of (n = NCEP) surface flux components ( *y* axis = W $m^{-2}$); and (c) outcome of heat budget calculations, demonstrating component influence ( *y* axis = sigma). Predicted SSTs vary less than observed.

the composite cases that is slightly larger. This yields a signal-to-noise ratio <1. Nonetheless, this slight increase creates a narrow opening between waters that are too cold to the north and a Coriolis value that is too small to the south. Another noteworthy point in the SST difference maps is the large area of near-zero values east and west of Florida. The SST signal lies farther south and east for Caribbean hurricanes than for all Atlantic hurricanes. The concept we gain from this understanding is an ''African gateway,'' whereby reduced upwelling off the west coast of Africa zonally widens the area of high thermodynamic energy available for hurricane genesis. There are relatively strong subsurface ocean signals in the SODA UMD composites (not shown) that indicate the thermocline anomaly across the tropical Atlantic deepens to the east during years of high CHD. Such an anomalous structure helps spread the thermodynamic energy that is usually concentrated in the west Atlantic eastward toward Africa. This, in turn, creates conditions for longer-lived hurricanes that track westward in lower latitudes (García-Herrera et al. 2006).

A feature of our SST composite analysis is the opposite sign of anomalies in the tropical east Pacific and the tropical Atlantic (Figs. 2a,b). This is not an inherent mode of climate variability but rather an optimal configuration for hurricane development in the Caribbean. A cold equatorial Pacific (La Niña) and a warm North Atlantic conspire to reduce wind shear over the Caribbean (favorable for hurricanes). However, warm Atlantic years seldom coincide with an ENSO extreme (Wang et al. 2006); SST anomalies in the two oceans tend to oscillate independently (Czaja et al. 2002; Wang et al. 2006). The shape of warm anomalies in the North Atlantic is consistent with that found by Frankignoul and Kestenare (2005) generated by the anomalous displacement of the subtropical high and positive air–sea feedback.

Figure 3 illustrates how the ENSO and tropical North Atlantic (TNA) influences on vertical wind shear differ during the Atlantic hurricane season (June–November). SST in the TNA is related to the size of the AWP. Figures 3a,c shows the 200- and 850-hPa geopotential height and wind vector differences, whereas Fig. 3e illustrates the zonal wind shear for the composite largest minus smallest

terciles of the AWP (from NCEP reanalysis). For comparison, Figs. 3b,d,f shows the composite maps for the cool minus warm terciles of Niño-3 SST. Both are characterized by easterly shear anomalies in the Caribbean, which is favorable for tropical cyclone development, but with differing distributions over the MDR. In agreement with Wang et al. (2006), the AWP response is an anomalous anticyclone (cyclone) at 200 (850) hPa north of the Caribbean (Figs. 3a,c), which produce the easterly shear anomaly (Fig. 3e). The ENSO composite has paired anticyclones at 200 hPa (Fig. 3b) straddling the Niño-3 region in the Pacific and an equatorial swath of reduced shear extending toward Africa (Fig. 3f). These patterns correspond to the Gill (1980) atmosphere response to off-equatorial and equatorial heating anomalies, respectively. They provide dynamical evidence for the relative independence of the Pacific and Atlantic composite SST features in Fig. 2, because they affect shear over the Caribbean.

The maximum potential intensity (MPI) index is the difference between SST and tropopause temperature, thus analyzed here. In Figs. 4a,b, the tropopause temperature field reveals a convectively cooled zone over west Africa in the preseason that expands westward along 20°N to the Caribbean at a phase speed of $-0.3$ m s$^{-1}$. The difference in tropopause temperature between high and low CHD years is ~1°C. As the cool zone at the tropopause extends westward across the tropical North Atlantic, an opposing warm zone develops along 10°S, indicating subsidence there. Klotzbach and Gray (2003) consider the southern feature as an indicator of hurricane activity. Tropopause temperatures reflect atmospheric thickness, so Fig. 4b is indicative of a thermal wind relationship between baroclinic changes north and south of the MDR and the vertical shear of zonal wind over the MDR itself. The observed relationship is consistent with lower (higher) MDR shear during periods of increased (decreased) Caribbean hurricane activity.

To more closely study this meridional feature, we analyze satellite OLR differences for a reduced set of composite cases. A sequence of two-monthly composite maps (Figs. 5a–d) reveals that the Atlantic ITCZ becomes more active as it shifts northward prior to active Caribbean hurricane seasons. The ITCZ extends more strongly into the Amazon basin from March to June. By July, the anomalous convection has continued northward from the equator to 15°N. This feature splits into two cells, a West African monsoon and a Caribbean node. By September, convective differences are greatest north of Venezuela where SSTs rise in conjunction with reduced evaporative fluxes (cf. Fig. 2b). There, a weakening of trade winds accompanies an enlarged Atlantic warm pool (Wang et al. 2006).

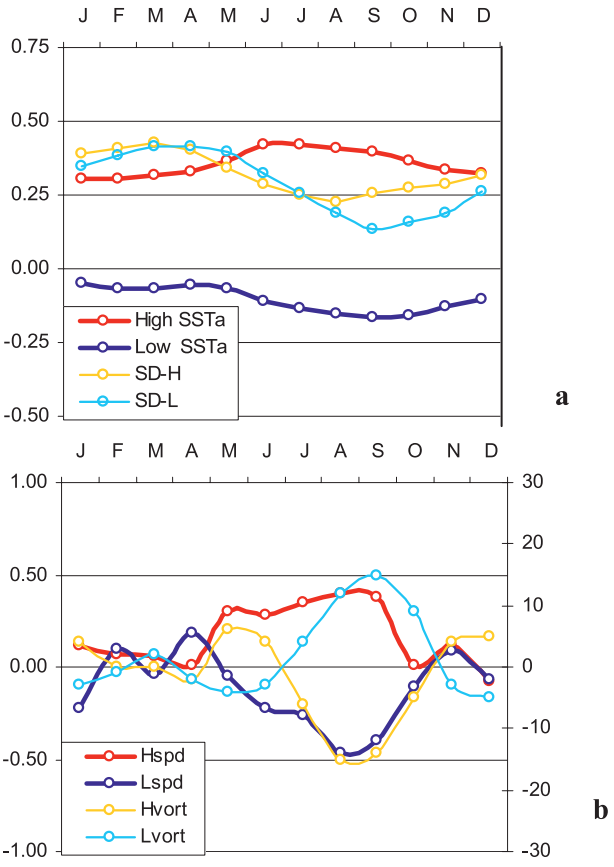


FIG. 8. (a) Composite and standard deviation of SST (°C) in the MDR for months preceding high and low hurricane seasons. (b) As in (a), but for composite wind speed and wind stress curl (labeled vort.). Both are inverted to account for their effect on SST, with units of (left) m s$^{-1}$ and (right) s$^{-1}$ 10$^{-6}$.

Given this sequence, we postulate that the Atlantic decadal and meridional signals are transmitted to Caribbean hurricanes through an energized Hadley circulation and ITCZ combined with MDR wind shear reduced by changes in meridional baroclinicity. We investigate the kinematic forcing to determine whether the northern or southern Hadley cell is most influential by analysis of composite vertical north–south section of divergent meridional wind and vertical motion in Figs. 6a,b. The difference field in MDR longitudes 25°–50°W during preseason reveals northerly anomalies in the latitudes 5°S–5°N in the lower layer. In the preseason, upper divergent flow is symmetrical over the equator, and the preseason upper northerly flow south of the equator spreads to 15°N during the hurricane season, where strong uplift is found. Sinking motions are evident in both seasons south of 10°S. Hence, meridional overturning is prevalent south of the hurricane track, which is in agreement with Wang and Enfield (2003) and Wang et al. (2006). With an intensified ITCZ, latent

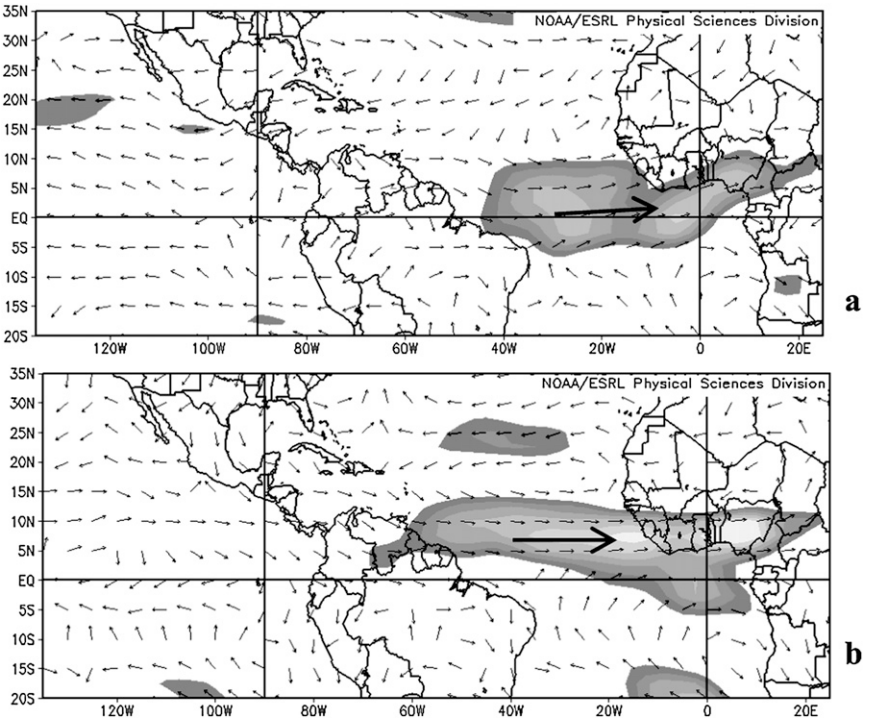


FIG. 9. (a) Preseason high minus low composite for 700-hPa wind field and (b) in-season 700-hPa wind field. Shading is at 0.2 m $s^{-1}$ intervals from 1.5.

heating increases atmospheric thickness; through the thermal wind relationship, vertical shear is reduced over the MDR. According to the caveats of Swanson (2008), the in-season convection at 15°–20°N may be as much a consequence of increased tropical storm activity as a cause of it.

### c. MDR ocean heat budget analysis

Given the importance of small changes in MDR SST to Caribbean hurricane activity, we analyze the heat budget and ask the following question: Which component of the heat budget is most effective in driving changes in SST with respect to CHD? We analyze the surface flux components: net solar insolation, outgoing radiation, evaporation, and sensible heating; the oceanic mixed layer advection; and the entrainment of cooler water from below. The heat budget climatology of the MDR is shown in Fig. 7a. The solar insolation has the greatest input, but its interannual variability is about half that of evaporation (Fig. 7b). Upwelling near Africa combined with a mean westward ocean current provides advective cooling, but that is overpowered by solar insolation. The net effect is a westward increase of sea temperature in the mixed layer from 23°C at 25°W to 26°C at 50°W and a simultaneous westward increase in rainfall rate from 1 to 2 mm $day^{-1}$.

Although the climatological results are straightforward, the interannual variability is somewhat ambiguous. Calculating the net surface flux, vertical entrainment, and horizontal advection, we obtain monthly predicted MDR SST. Figure 7c evaluates the different components of the heat budget. Surface fluxes (mainly evaporative) dominate over entrainment and advection, based on the standard deviations.

Using composite analysis, we find that SSTs are significantly higher in the MDR before and during active hurricane seasons, but standard deviations $\sigma$ are equally high amongst cases, contributing to the composite (Fig. 8a). Hence, individual members of the composite deviate by an amount that is as large as the difference between the low and high case means. The signal-to-noise ratio (difference divided by sigma) only improves after May. Thus, MDR SSTs in the spring months may not be a reliable predictor of subsequent Caribbean hurricanes and it is necessary to look farther upstream in the northwest Africa upwelling zone (dashed box in Fig. 2a). The composite MDR winds are analyzed in Fig. 8b (with sign of wind influence inverted to account for SST forcing) and reveal no significant differences prior to May. At least the wind stress curl (controlling vertical motion) cooperates with the wind speed influence on evaporation during May and June to produce warming (cooling) prior to active (inactive) seasons. During the hurricane season,

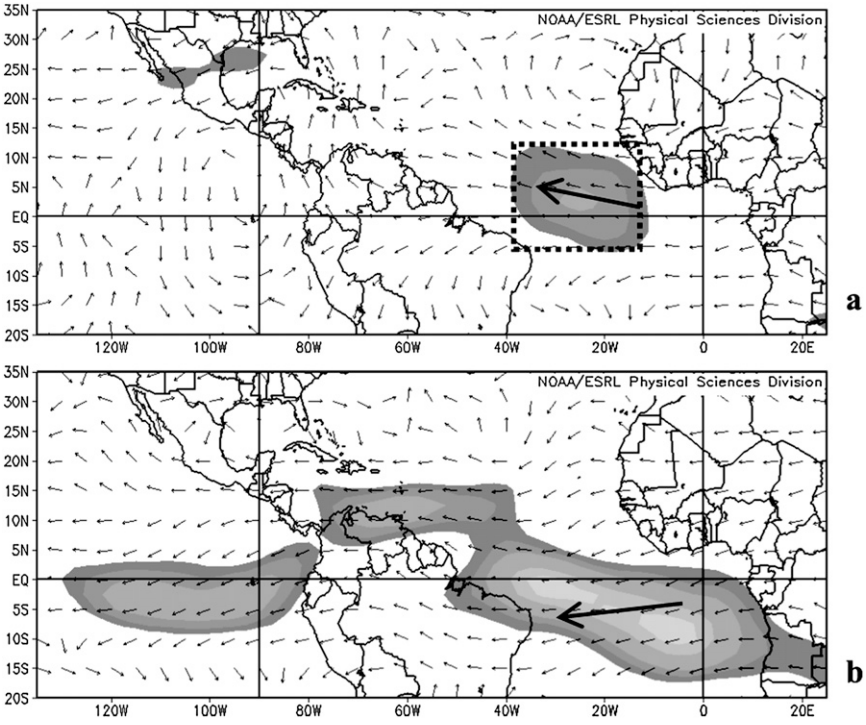


FIG. 10. (a) Preseason high minus low composite for 200-hPa wind field and (b) in-season 200-hPa wind field. Box in (a) refers to predictor used in model. Shading is at 0.5 m $s^{-1}$ intervals from 3.

the composite wind stress curl (difference) is cyclonic and cools the mixed layer. This process is opposed by warming through reduced evaporation and may explain why SST differences between high and low Caribbean hurricane years are relatively small, despite the 1 m $s^{-1}$ (20%) decrease in wind speed in August and September. Horizontal advective effects occur as upwelled water is drawn toward the MDR; however, there appears to be little influence on interannual SST anomalies. Statistical tests indicate that no single component dominates the heat budget. Although evaporative flux governs MDR SSTs during the hurricane season, it is an ambiguous predictor at seasonal lead times. In the following section, we study the kinematic drivers of Caribbean Hurricanes.

### *d. Composite kinematic structure*

The 700- and 200-hPa composite wind maps are shown in Figs. 9a,b and 10a,b. These difference maps reveal a zonal overturning circulation cell with enhanced lower westerlies (upper easterlies) between South America and West Africa with regard to high CHD. Zonal wind differences overlie convection, drifting northward together (cf. Figs. 5, 9). To study the Walker circulation anomaly in detail, we analyze a vertical east–west section composite of divergent zonal wind and vertical motion in Fig. 11. Low-level westerlies are drawn toward West Africa, whereas upper-level easterly flow extends across the east Atlantic. There is a single Walker anomaly in the preseason, with sinking motions over the Pacific (100°–140°W) complimenting rising motions in the West African monsoon (0°–20°W, Fig. 11a). During the hurricane season (Fig. 11b), the pattern breaks down into two cells (with sinking nodes at 130° and 60°W), and signals weaken, whereas the meridional circulation strengthens (Fig. 6b). As suggested by Figs. 6 and 11 together, both seasons are quite three dimensional rather than purely meridional or zonal. The westward spread of upper easterly flow anomalies coincides with a shift in the low-level velocity potential as indicated by a composite sequence (Hovmöller plot) in Fig. 12a. Convergent conditions shift toward the MDR, favoring the intensification of easterly waves coming off the West African coast.

This westward shift occurs with a phase speed of $-0.27$ m $s^{-1}$. The east Pacific cold tongue spreads slowly westward in our composite analysis (Figs. 2a,b), creating a region of sinking motion that draws upper-level flow from the Atlantic sector. Zonal propagation of equatorial Pacific SST anomalies depends on the overlying winds and Walker cells and can be in either direction (Wang 1995). Westward propagation is favored when subtropical ocean Rossby waves are more active (Huang 2004; Yeshanew and Jury 2007) and may influence the Atlantic

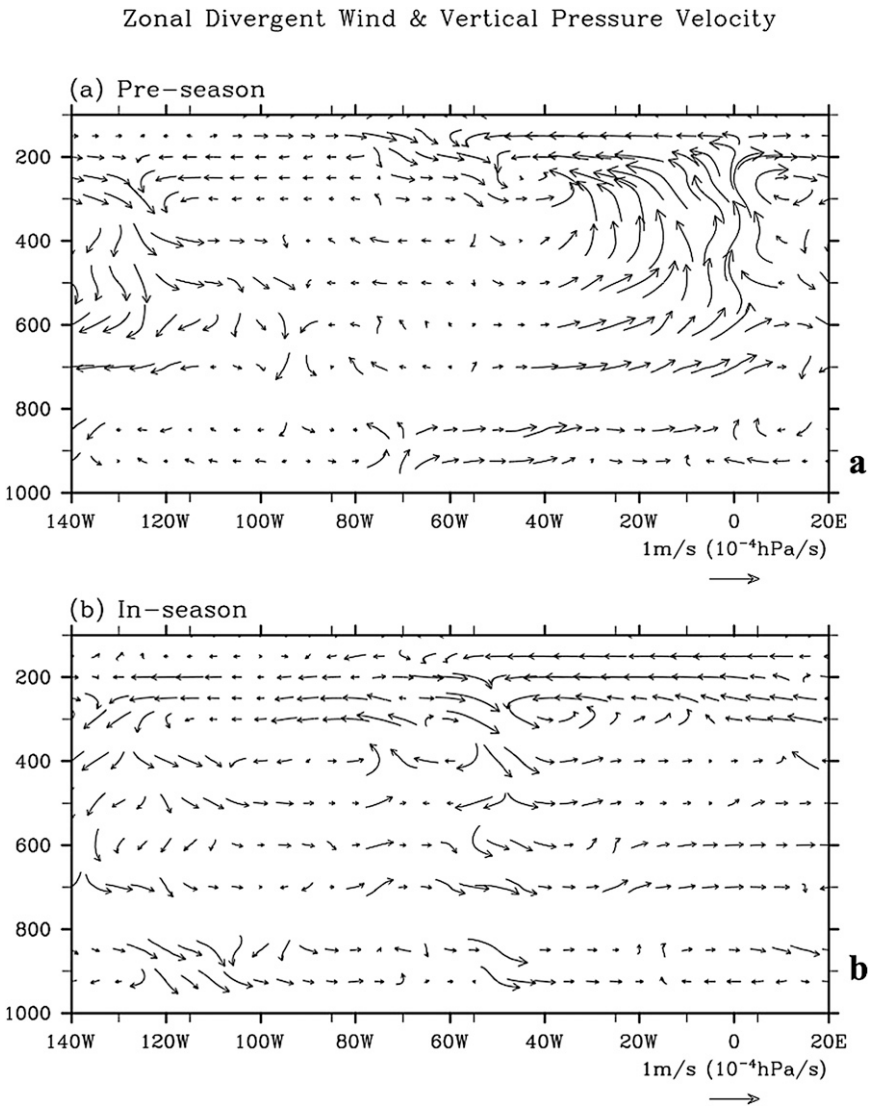


FIG. 11. Vertical east–west section composite over the equator (5°S–5°N) of divergent component of zonal wind and vertical motion (inverted omega scaled up × 100) during (a) preseason and (b) in-season. The vector key is given.

Walker circulation and Caribbean hurricanes through the shift of both MPI (SST − Ttrop; Figs. 2, 4) and convergence (Fig. 12a) from West Africa to the MDR. Another mechanism is expansion of the AWP and associated weakening of wind shear south of the hurricane path (Fig. 3b). Thus, two dynamical influences are juxtaposed, representing the Gill (1980) response to equatorial and off-equatorial heating anomalies, and together composite into westward propagation.

## 4. Discussion

Hurricanes that pass through the Caribbean tend to develop closer to Africa and have a more westward trajectory than their non-Caribbean counterparts. Surface air pressure composite maps (not shown) reveal an increase of air pressure over the southeast Pacific before and during the season. A separate region of low pressure shifts from the equatorial Atlantic to the Caribbean. The two opposing centers rotate counterclockwise from east–west to northeast–southwest orientation, possibly reflecting a gradual increase in Hadley cell influence as the season progresses.

There are various factors modulating tropical cyclone development in the Caribbean: vertical wind shear, thermodynamic energy (MPI), low-level stability and vorticity, African aerosols, etc. As shown in Fig. 3, shear anomalies may be created independently over the Caribbean and

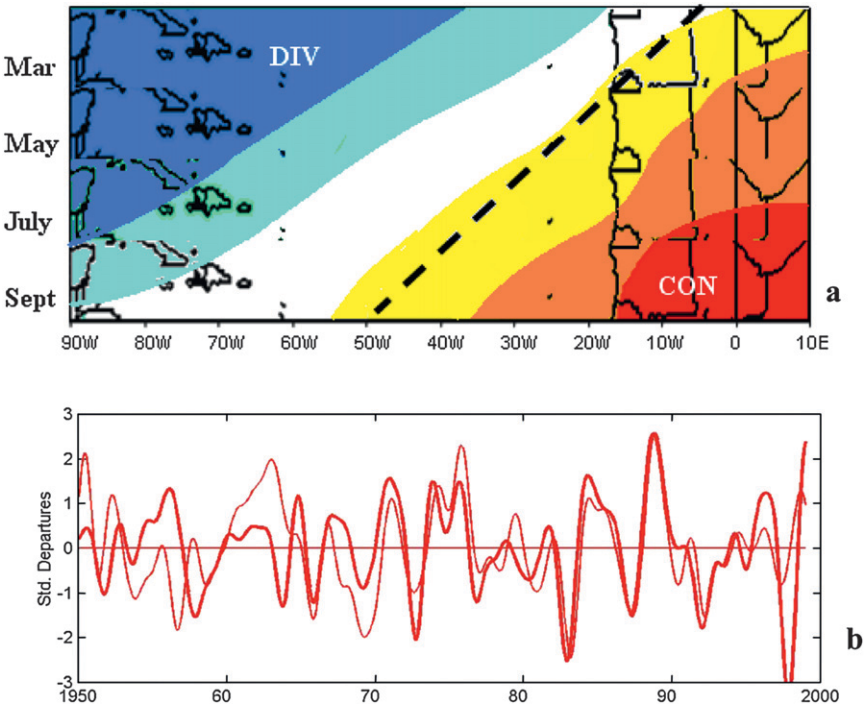


FIG. 12. (a) Successive strips of 15°–22°N band high minus low composite 850-hPa velocity potential, forming a Hovmöller plot. Shading is from $-1.2 \times 10^6$ (blue) to $+0.8 \times 10^6$ (red) interval $0.4 \times 10^6$ m$^2$ s$^{-1}$. Dashed line highlights westward shift of convergent region. (b) Comparison of equatorial Pacific zonal thermocline oscillation and equatorial Atlantic zonal wind shear (bold), with wavelet smoothing (from Yeshanew and Jury 2007).

MDR by Pacific ENSO and Atlantic warm pool SST. The concomitant intensification of meridional thermal gradients over the Atlantic confirms that the shear anomaly is in thermal wind balance (Fig. 4). The high minus low composite increase in low-level streamfunction in the tropical Atlantic (not shown) reflects the transformation of easterly waves into tropical cyclones. Hence, active Caribbean hurricane seasons are related to both reduced upper shear and low-level vorticity changes over the MDR and to adjustments in moist static energy (Wang and Lee 2007).

The question of competing influences on Caribbean hurricanes can be answered statistically through development of a simple algorithm that considers the various key predictors identified. Preseason SST and wind changes in the tropics and near Africa should offer useful forecasts of Caribbean hurricanes at three-month lead time. We evaluate predictability using forward stepwise multivariate linear regression of the CHD (target) against five candidate predictors in the period 1951–2005. The March–May predictors include stratospheric QBO, Pacific Niño-3SST, Atlantic AMO SST, northeast Atlantic (NEA) SST (box in Fig. 2a), and Atlantic zonal shear (U700–U200, box in Fig. 11a; zonal). Two possible outcomes are generated:

$$\text{CHD} = -0.34(\text{Niño} - 3) + 0.61(\text{AMO}), \quad r^2 = 0.34,$$
$$\text{standard error} = 0.81 \quad \text{and}$$

$$\text{CHD} = +0.51(\text{NEA}) + 0.38(\text{zonal}), \quad r^2 = 0.32,$$
$$\text{standard error} = 0.82.$$

The first algorithm (cf. Fig. 13) reflects the impact of ENSO on wind shear and regional surface heat supply through Atlantic SST. The second algorithm considers SST in the northwest African upwelling region and the Atlantic zonal overturning (Walker) cell. Statistical tests reveal that each predictor is valuable ($p = 0.0002$ for AMO, $p = 0.0080$ for Niño-3, $p = 0.0004$ for NEA, and $p = 0.0014$ for zonal). In both algorithms, the predictor related to Atlantic SST has the largest influence, and both achieve one-third of variance for Caribbean hurricane days in a 1 June forecast.

Another question to be posed is whether Caribbean hurricanes are enhanced by environmental conditions

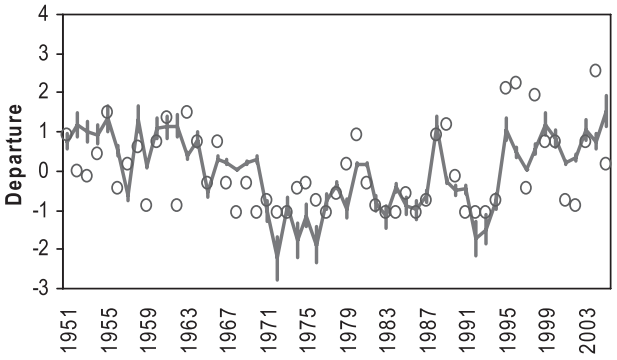


FIG. 13. Outcome of a multivariate model at 3-month lead time to predict Caribbean hurricane days from AMO and Niño-3: predicted (with error bars) vs observed (open dots).

any different than for hurricanes in the wider Atlantic. Constructing SST and wind composites based on the HRD accumulated cyclone energy (ACE) index, we find the Pacific cold anomaly and Walker overturning is stronger and farther west for Atlantic hurricanes. Otherwise, environmental conditions are similar.

## 5. Summary

Our analysis shows that the conditioning of Caribbean hurricane activity is consistent with that for the wider Atlantic basin. Composite analyses of environmental conditions based on high minus low hurricane activity in the Caribbean confirm an influence from both Pacific ENSO and the tropical North Atlantic. When considered in respect to seasonal hurricanes, the two factors provide distinct inputs, although MDR SSTs may sometimes inherit anomalies from an earlier ENSO event. ENSO kinematically affects the Caribbean season through the vertical wind shear because of a concurrent atmospheric response to Pacific SST anomalies. The Atlantic warm pool size (extension into the MDR) affects the shear also, as well as the moist static stability, but the large-scale atmospheric response pattern differs from that of ENSO: it corresponds with a Gill atmosphere response to an off-equatorial heating anomaly centered in the Caribbean. Using contingency tables and regression equations, the remote (ENSO) and in-region (AWP) indices both show statistical skill to replicate Caribbean hurricane activity index at a 3–6-month lead. However, Atlantic SST holds greater overall influence and skill.

The atmospheric composites reveal interesting zonal migrations of anomalies between the preseason and in-season periods. In the case of remote forcing, this could possibly be a response of the atmospheric overturning circulation to a westward expanding cold tongue anomaly in the Pacific. In the case of Atlantic forcing, it may reflect the increase in the impact of developing SST anomalies, because absolute SSTs in the Caribbean rise during boreal summer. However, our analysis does not separate these possibilities, because the distinct Pacific and Atlantic forcings are ''blended'' in the composites and ''frozen'' in time and space, whereas in reality they are likely to have a variable influence. The migrating patterns indicate that precursor conditions in the spring have predictive skill for the ensuing hurricane season at least for 3-month lead forecasts, given the late arrival of a respectable signal-to-noise ratio.

*Acknowledgments.* The first author acknowledges NSF Epscor support for research on Caribbean hurricanes at the Physics Department, University of Puerto Rico, Mayaguez.

## REFERENCES

Aiyyer, A. R., and C. Thorncroft, 2006: Climatology of vertical wind shear over the tropical Atlantic. *J. Climate,* **19,** 2969–2983.

Carton, J. A., B. S. Giese, X. Cao, and L. Miller, 1996: Impact of altimeter, thermistor, and expendable bathythermograph data on retrospective analyses of the tropical Pacific Ocean. *J. Geophys. Res.,* **101,** 14 147–14 159.

Chang, P., L. Ji, and H. Li, 1997: A decadal climate variation in the tropical Atlantic Ocean from thermodynamic air-sea interaction. *Nature,* **385,** 516–518.

Cook, K. H., J. S. Hsieh, and S. M. Hagos, 2004: The Africa–South America intercontinental teleconnection. *J. Climate,* **17,** 2851–2865.

Czaja, A., P. van der Vaart, and J. Marshall, 2002: A diagnostic study of the role of remote forcing in tropical Atlantic variability. *J. Climate,* **15,** 3280–3290.

Elsner, J. B., and T. H. Jagger, 2008: United States and Caribbean tropical cyclone activity related to the solar cycle. *Geophys. Res. Lett.,* **35,** L18705, doi:10.1029/2008GL034431.

——, R. J. Murnane, and T. H. Jagger, 2006: Forecasting U.S. hurricanes 6 months in advance. *Geophys. Res. Lett.,* **33,** L10704, doi:10.1029/2006GL025693.

Enfield, D. B., and S.-K. Lee, 2005: The heat balance of the Western Hemisphere warm pool. *J. Climate,* **18,** 2662–2681.

——, ——, and C. Wang, 2006: How are large Western Hemisphere warm pools formed? *Prog. Oceanogr.,* **70,** 346–365.

Frankignoul, C., and E. Kestenare, 2005: Air–sea interactions in the tropical Atlantic: A view based on lagged rotated maximum covariance analysis. *J. Climate,* **18,** 3874–3890.

García-Herrera, R., L. Gimeno, P. Ribera, E. Hernández, E. González, and G. Fernández, 2006: Identification of Caribbean basin hurricanes from Spanish documentary sources. *Climatic Change,* **83,** 55–85.

Gill, A. E., 1980: Some simple solutions for heat-induced tropical circulation. *Quart. J. Roy. Meteor. Soc.,* **106,** 447–462.

Goldenberg, S. B., and L. J. Shapiro, 1996: Physical mechanisms for the association of El Niño and West African rainfall with Atlantic major hurricane activity. *J. Climate,* **9,** 1169–1187.

——, C. W. Landsea, C. W. Mestas-Nuñez, and W. M. Gray, 2001: The recent increase in Atlantic hurricane activity: Causes and implications. *Science,* **293,** 474–479.

Gray, W. M., 1984: Atlantic seasonal hurricane frequency. Part I: El Niño and 30 mb quasi-biennial oscillation influences. *Mon. Wea. Rev.,* **112,** 1649–1668.

Hastenrath, S., 2000: Interannual and longer term variability of upper-air circulation over the tropical Atlantic and West Africa in boreal summer. *Int. J. Climatol.,* **20,** 1415–1430.

Hopsch, S. B., C. D. Thorncroft, K. Hodges, and A. Aiyyer, 2007: West African storm tracks and their relationship to Atlantic tropical cyclones. *J. Climate,* **20,** 2468–2483.

Huang, B., 2004: Remotely forced variability in the tropical Atlantic Ocean. *Climate Dyn.,* **23,** 133–152.

Jury, M. R., 2003: Coherent variability of African River flows, composite climate structure and the Atlantic circulation. *Water S.A.,* **29,** 1–10.

——, 2009: A quasi-decadal cycle in Caribbean climate. *J. Geophys. Res.,* **114,** D13102, doi:10.1029/2009JD011741.

——, D. B. Enfield, and J.-L. Mélice, 2002: Tropical monsoons around Africa: Stability of El Niño–Southern Oscillation associations and links with continental rainfall. *J. Geophys. Res.,* **107** (C10), 1–17.

Klotzbach, P. J., and W. M. Gray, 2003: Forecasting September Atlantic basin tropical cyclone activity. *Wea. Forecasting,* **18,** 1109–1128.

Knaff, J. A., 1997: Implications of summertime sea level pressure anomalies in the tropical Atlantic region. *J. Climate,* **10,** 789–804.

Landsea, C. W., 2007: Counting Atlantic tropical cyclones back to 1900. *Eos, Trans. Amer. Geophys. Union,* **88,** doi:10.1029/2007EO180001.

——, B. A. Harper, K. Hoarau, and J. A. Knaff, 2006: Can we detect trends in extreme tropical cyclones? *Science,* **313,** 452–454.

Maloney, E. D., and D. L. Hartmann, 2000: Modulation of hurricane activity in the Gulf of Mexico by the Madden-Julian oscillation. *Science,* **287,** 2002–2004.

Mestas-Nuñez, A. M., and D. B. Enfield, 2001: Eastern equatorial Pacific SST variability: ENSO and non-ENSO components and their climatic associations. *J. Climate,* **14,** 391–402.

Nyberg, J., B. Malmgren, A. Winter, M. R. Jury, H. Kilbourne, and T. Quinn, 2007: Low Atlantic hurricane activity in the 1970s and 1980s compared to the past 270 years. *Nature,* **447,** 698–701.

Swanson, K. L., 2008: False causality between Atlantic hurricane activity fluctuations and seasonal lower atmospheric wind anomalies. *Geophys. Res. Lett.,* **35,** L18807, doi:10.1029/2008GL034469.

Wang, B., 1995: Interdecadal changes in El Niño onset in the last four decades. *J. Climate,* **8,** 267–285.

Wang, C., and D. B. Enfield, 2003: A further study of the tropical Western Hemisphere warm pool. *J. Climate,* **16,** 1476–1493.

——, and S.-K. Lee, 2007: Atlantic warm pool, Caribbean low-level jet, and their potential impact on Atlantic hurricanes. *Geophys. Res. Lett.,* **34,** L02703, doi:10.1029/2006GL028579.

——, D. B. Enfield, S.-K. Lee, and C. W. Landsea, 2006: Influences of the Atlantic warm pool on Western Hemisphere summer rainfall and Atlantic hurricanes. *J. Climate,* **19,** 3011–3028.

——, S.-K. Lee, and D. B. Enfield, 2007: Impact of the Atlantic warm pool on the summer climate of the Western Hemisphere. *J. Climate,* **20,** 5021–5040.

——, ——, and ——, 2008: Atlantic warm pool acting as a link between the Atlantic multidecadal oscillation and Atlantic tropical cyclone activity. *Geochem. Geophys. Geosyst.,* **9,** Q05V03, doi:10.1029/2007GC001809.

Xie, S.-P., and S. G. H. Philander, 1994: A coupled ocean-atmosphere model of relevance to the ITCZ in the eastern Pacific. *Tellus,* **46A,** 340–350.

Yeshanew, A., and M. R. Jury, 2007: North African climate variability. Part 1: Tropical thermocline coupling. *Theor. Appl. Climatol.,* **89,** 25–36, doi:10.1007/s00704-006-0242-8.

Yu, L., M. M. Rienecker, and B. Sun, 2004: Improving latent and sensible heat flux estimates for the Atlantic Ocean (1988–99) by a synthesis approach. *J. Climate,* **17,** 373–393.